Archives

Ref.TH.1883-CERN

ELECTROMAGNETIC CORRECTIONS TO THE INDUCED PSEUDOSCALAR TERM IN NUCLEAR MUON CAPTURE *)

L.P. Fulcher

Department of Physics and Astronomy
University of Maryland, College Park
Maryland 20742, U.S.A.
and
Department of Physics
Bowling Green State University
Bowling Green, Ohio 43403, U.S.A. **)

and

M. C. Mukhopadhyay

Center for Theoretical Physics +)
University of Maryland, College Park
Maryland 20742, U.S.A.
and
CERN -- Geneva **)
Switzerland

A B S T R A C T

We study the electromagnetic correlations to the induced pseudoscalar term in nuclear muon capture. The effects of the static nuclear magnetic field are shown to be very small. We calculate the effects of the nuclear Coulomb field by constructing the Green's function appropriate for pions moving in the Coulomb field of an extended nucleus and using realistic muon wave functions. Consideration of finite nuclear size is shown to be imperative in order to obtain accurate results. The Coulomb corrections are not large enough to play any significant rôle in understanding the discrepancy of the theory with the recent measurement of the photon spectrum following radiative muon capture in ^{40}Ca or of the rate of the reaction $^{16}O(\mu^-,\nu_\mu)^{16}N(0^-)$. Two approximate methods of obtaining the results are also presented.

---

*) Supported in part by the US Atomic Energy Commission and the National Science Foundation for the portion of the work done at the University of Maryland.

**) Present address.

+) Center for Theoretical Physics Postdoctoral Fellowship.

Ref.TH.1883-CERN
20 June 1974

1. INTRODUCTION

Much of the theoretical studies*) dealing with nuclear muon capture have been based on the impulse approximation. In these works the value used for the induced pseudoscalar coupling constant C_p **) has usually been that obtained by assuming the divergence of the axial-vector current to be dominated by the pion pole term[3] (PCAC). This value is consistent with the recent muon capture experiment done with hydrogen[4]. However, experimental evidence supporting the use of the PCAC value in complex nuclei is difficult to obtain, since questions[5] about nuclear structure inevitably accompany any attempt to extract weak interaction coupling constants from muon capture data. For example, the analyses of the allowed transitions in light nuclei[5] are consistent with the PCAC value, but they do not rule out a substantial deviation from this result. The recent measurement[6] of the β-decay rate of the ^{16}N (0^-:120 keV) state to the ground state of ^{16}O, together with the currently available two different values[7,8] of the rate of $^{16}O_{gs}$ $(\mu^-,\nu_\mu)^{16}N(0^-)$ transition, allows us to determine the value of C_p nearly independently of the nuclear model uncertainties. This analysis[6] yields a value of C_p substantially larger than the PCAC prediction. Furthermore, the most recent measurement[9] of the photon spectrum from the radiative muon capture on ^{40}Ca is completely inconsistent with the PCAC predictions.

In view of these experiments and the lack of convincing experimental support for using the PCAC value for C_p in complex nuclei, we feel that it is important to study carefully the propagation of off-mass-shell pions in complex nuclei. The fact that other corrections[10] (such as 'real' or 'induced' second-class effects) may be equally important does not make this study any less compelling.

In this work***) we consider only the influence of the nuclear electromagnetic field on the induced pseudoscalar term, postponing until later a discussion of the effects of nuclear strong interactions[12]. Our effort is based on a theorem which was first proved by Baba[13]. The theorem is reviewed in Section 2, and its relation to Blokhintsev and Dolinsky's observation[14] is discussed. The Klein-Gordon equation and the generalization of the muon capture formalism necessary to include the electromagnetic corrections are subjects of Section 3. In Section 4, we present numerical results and point out the necessity of considering finite nuclear size in order to obtain reliable results. Our results differ substantially from those obtained by Baba[13], who treated the nucleus as a point charge. In Section 5, we discuss in considerable detail several approximate methods of obtaining some of the numerical results presented in Section 4, and we summarize our conclusions in Section 6.

---

*) For a review of these works, see Refs. 1.

**) See Ref. 2 for the definition C_p used in this paper. It is called g_2 in this reference.

***) Preliminary accounts of this work are given in Refs. 11.

2. THE THEOREM

We begin by introducing the scattering matrix element for the induced pseudoscalar part of muon capture on a proton, namely,

$$S_{fi} = \langle \nu n | \hat{S} | \mu^- p \rangle , \tag{1}$$

where the labels on the initial and final states refer to the particles present. In establishing the theorem we use a simple model of the pion-nucleon interaction which, to lowest order in the pion-nucleon coupling constant, is equivalent to the assumption of pion pole dominance. The theorem is most readily proved by working in an interaction picture[15] where the unperturbed Hamiltonian H_0 is chosen to include the effects of the nuclear electromagnetic potentials A_λ. It leads to the equations of motion*),

$$\left[\gamma_\lambda \left(\frac{\partial}{\partial x_\lambda} - ie A_\lambda\right) + m_\mu\right] \psi_\mu = 0, \tag{2}$$

$$\left[\left(\frac{\partial}{\partial x_\lambda} - ie A_\lambda\right)^2 - m_\pi^2\right] \phi_\pi = 0, \tag{3}$$

for the muon field operator ψ_μ and the pion field operator ϕ_π. In these equations e is equal to the charge of the negative muon, and the quantities γ_λ are the usual Dirac matrices. The perturbation includes three terms,

$$H' = V_1 + V_2 + V_3 , \tag{4}$$

where

$$V_1 = i\sqrt{2}\, g_\pi \int d^3x\, \phi_\pi(x)\, \bar{\psi}_n(x)\, \gamma_5\, \psi_p(x), \tag{5}$$

$$V_2 = i G \frac{f_\pi}{\sqrt{2}} \int d^3x\, \bar{\psi}_\nu(x)\,(1-\gamma_5)\,\gamma_5\,\gamma_\lambda\,\psi_\mu(x) \frac{\partial}{\partial x_\lambda} \phi_\pi^\dagger(x), \tag{6}$$

$$V_3 = -\frac{G e f_\pi}{\sqrt{2}} \int d^3x\, \bar{\psi}_\nu(x)\,(1-\gamma_5)\gamma_5\,\gamma_\lambda\,\psi_\mu(x)\, A_\lambda(x)\, \phi_\pi^\dagger(x), \tag{7}$$

Here g_π is the pseudoscalar pion-nucleon coupling constant, G is the weak interaction coupling constant, and f_π is the pion decay constant. The second term is the Hermitian conjugate of an effective Hamiltonian that describes negative pion decay. The third term is a seagull term which arises from the minimal substitution,

$$\frac{\partial}{\partial x_\lambda} \phi_\pi^\dagger \rightarrow \left(\frac{\partial}{\partial x_\lambda} + ie A_\lambda\right) \phi_\pi^\dagger , \tag{8}$$

in the second term. It is necessary in order to satisfy gauge invariance.

---

*) Units are such that $\hbar = c = 1$.

The second-order scattering operator is given by

$$\hat{S}^{(2)} = -\frac{1}{2} \int_{-\infty}^{\infty} dt \int_{-\infty}^{\infty} dt' \, T\left[H'(t) \, H'(t') \right], \tag{9}$$

where T denotes the time-ordered product[15]. Using Eqs. (4)-(7) we find that

$$S_{fi}^{(2)} = g_\pi G f_\pi \int d^4x \int d^4x' \langle f | T \{ \phi_\pi(x) \, \bar{\Psi}_n(x) \gamma_5 \Psi_p(x) \times \bar{\Psi}_\nu(x') (1-\gamma_5) \gamma_5 \gamma_\lambda \Psi_\mu(x') \times \left(\frac{\partial}{\partial x'_\lambda} + ie \, A(x') \right) \phi_\pi^+(x') \} | i \rangle . \tag{10}$$

This expression leads to the two graphs which are shown in Fig. 1. There the wave functions and propagators of all charged particles are those appropriate for the nuclear electromagnetic field. Integrating Eq. (10) by parts in the variable x', we have

$$S_{fi}^{(2)} = g_\pi G f_\pi \int d^4x \int d^4x' \langle f | T \{ \phi_\pi(x) \, \bar{\Psi}_n(x) \gamma_5 \Psi_p(x) \times \phi_\pi^+(x') \left(-\frac{\partial}{\partial x'_\lambda} + ie \, A(x') \right) \bar{\Psi}_\nu(x') (1-\gamma_5) \gamma_5 \gamma_\lambda \Psi_\mu(x') \} | i \rangle . \tag{11}$$

In this equation there is no term which arises from differentiating the T operator, since this term contains the equal-time commutator of $\phi_\pi(x)$ with $\phi_\pi^+(x')$, which is equal to zero. To proceed further we note that the action of the differential operator $\partial/\partial x'_\lambda$ leads to two expressions which can be evaluated with the aid of the equations of motion for $\bar{\psi}_\nu(x')$ and $\psi_\mu(x')$ [see Eq. (2)]. Thus

$$S_{fi}^{(2)} = C \int d^4x \int d^4x' \langle f | T \{ \phi_\pi(x) \, \bar{\Psi}_n(x) \gamma_5 \Psi_p(x) \times \phi_\pi^+(x') \, \bar{\Psi}_\nu(x') (1-\gamma_5) \gamma_5 \gamma_\lambda \Psi_\mu(x') \} | i \rangle , \tag{12}$$

where $C = g_\pi G f_\pi m_\mu$. Introducing the pion propagator,

$$G(x, x') = -i \langle 0 | T (\phi_\pi(x), \, \phi_\pi^+(x')) | 0 \rangle , \tag{13}$$

where $|0\rangle$ denotes the vacuum state, and using the same notation for the Fermion wave functions as for the field operators, we have that

$$S_{fi}^{(2)} = i \, C \int d^4x \int d^4x' \, \bar{\Psi}_n(x) \gamma_5 \Psi_p(x) \, G(x, x') \times \bar{\Psi}_\nu(x') (1-\gamma_5) \gamma_5 \Psi_\mu(x') . \tag{14}$$

This equation embodies the theorem[13]. This implies that the contribution of the graph with the seagull term in Fig. 1 is cancelled by part of the contribution from the other graph.

Blokhintsev and Dolinsky[14] noted that the effective Hamiltonian for the induced pseudoscalar term,

$$H_{ps} = -\frac{g_2 G}{\sqrt{2}} \int d^3x\, \bar{\Psi}_n(x)\gamma_5\Psi_p(x)\frac{\partial}{\partial x_\lambda}\bar{\Psi}_\nu(x)(1-\gamma_5)\gamma_5\gamma_\lambda\Psi_\mu(x), \tag{15}$$

where g_2 is the induced pseudoscalar form factor, is not gauge invariant unless one makes the minimal substitution

$$\frac{\partial}{\partial x_\lambda} \longrightarrow \frac{\partial}{\partial x_\lambda} - ie A_\lambda ,$$

a point not previously appreciated by Tadić[16]. Some clarification regarding the use of the minimal substitution in Eq. (15) is in order here, since it is perhaps unclear to which degrees of freedom the derivative there refers. The form of Eq. (11) clearly suggests that this derivative refers to the muonic degrees of freedom, thus clarifying the choice of sign in the minimal substitution. Of course, no uncertainty accompanies the minimal substitution of Eq. (8), since the derivative there clearly refers to the pionic degrees of freedom. Finally, we note that the effective Hamiltonian in Eq. (15) does not make it clear whether the pion propagator should be modified by the nuclear electromagnetic field since the pion field does not appear there explicitly.

3. THE KLEIN-GORDON EQUATION AND THE MUON CAPTURE FORMALISM

From the definition of the Green's function [Eq. (13)] and Eq. (3) we may obtain the equation of motion for the pion Green's function; that is,

$$\left[\left(\frac{\partial}{\partial x_\lambda} - ie A_\lambda\right)^2 - m_\pi^2\right] G(x,x') = \delta(\underset{\sim}{x}-\underset{\sim}{x}')\,\delta(t-t'). \tag{16}$$

If the pion field interacts only with a static Coulomb potential V_c, then after separating the time dependence from Eq. (16) we have

$$\left[\nabla^2 + (E_\pi - V_c)^2 - m_\pi^2\right] G_{E_\pi}(\underset{\sim}{x},\underset{\sim}{x}') = \delta(\underset{\sim}{x}-\underset{\sim}{x}'), \tag{17}$$

where E_π is the energy carried by the pion field. It is equal to the difference between the muon and the neutrino energies. In the next section we show that the effects of the nuclear magnetic field are small in comparison with those of the nuclear Coulomb field. Restricting our discussion to the case of spherically symmetric Coulomb potentials, we may separate the angular dependence from the radial dependence. This separation takes the form[17],

$$G_{E_\pi}(\underset{\sim}{x},\underset{\sim}{x}') = \sum_{l,m} Y^*_{lm}(\hat{x}')\, Y_{lm}(\hat{x})\; g_l(x,x'), \tag{18}$$

where the quantities $Y_{\ell m}(\hat{x})$ are the spherical harmonics of order ℓ, and g_ℓ satisfies the radial equation

$$\left[\frac{1}{x}\frac{d^2}{dx^2}x - \frac{l(l+1)}{x^2} + (E_\pi - V_c)^2 - m_\pi^2\right] g_l(x,x') = \frac{\delta(x-x')}{x^2}. \tag{19}$$

We discuss the numerical solution of this equation in the next section.

Assuming that all of the wave functions appearing in Eq. (14) are eigenstates of the appropriate Hamiltonians, the scattering matrix element may be written

$$S^{(2)}_{fi} = 2\pi i\, C\, \delta(E_n + E_\nu - E_\mu - E_p) \int d^3x \int d^3x'\, G_{E_\pi}(\underset{\sim}{x},\underset{\sim}{x}') \times \bar{\Psi}_n(\underset{\sim}{x})\gamma_5\Psi_p(\underset{\sim}{x})\,\bar{\Psi}_\nu(\underset{\sim}{x}')(1-\gamma_5)\gamma_5\Psi_\mu(\underset{\sim}{x}'). \tag{20}$$

In order to discuss the corrections in a manner independent of any nuclear model, we introduce a function $F(\underset{\sim}{x})$ such that

$$F(\underset{\sim}{x})\bar{\Psi}_\nu(\underset{\sim}{x})(1-\gamma_5)\psi_\mu(\underset{\sim}{x}) = -(\kappa^2+\nu^2)\int d^3x'\, G_{E_\pi}(\underset{\sim}{x},\underset{\sim}{x}')\,\bar{\Psi}_\nu(\underset{\sim}{x}')(1-\gamma_5)\psi_\mu(\underset{\sim}{x}'), \tag{21}$$

where $\kappa^2 = m_\pi^2 - E_\pi^2$ and ν is the magnitude of the neutrino momentum. In general F is a matrix in the space of the Dirac spinors. If the muon wave function is taken to be that for a free particle with zero momentum and the pion propagator is taken to be that for a free particle, then $F(\underset{\sim}{x}) = 1$, the value generally used in impulse approximation calculations. The dependence upon the argument $\underset{\sim}{x}$ allows for the variation of the correction over the nuclear volume and a dependence of the correction on the neutrino angular momentum. In our calculations we consider only the non-relativistic limit of Eq. (21). We take the relativistic muon wave function there to be the product of a non-relativistic wave function (also denoted as ψ_μ) and a free particle muon spinor. In this limit the definition of $F(\underset{\sim}{x})$ may be written as

$$F(\underset{\sim}{x})\,e^{-i\underset{\sim}{\nu}\cdot\underset{\sim}{x}}\,\psi_\mu(x) = -(\kappa^2+\nu^2)\int d^3x'\, G_{E_\pi}(\underset{\sim}{x},\underset{\sim}{x}') \times e^{-i\underset{\sim}{\nu}\cdot\underset{\sim}{x}'}\,\psi_\mu(\underset{\sim}{x}'). \tag{22}$$

Although one can calculate the function F exactly from this equation, the form of the correction in Eq. (22) is not the most convenient one from the point of view of nuclear model calculations. Thus we introduce $D(\underset{\sim}{x}) \equiv F(\underset{\sim}{x})\, e^{-i\underset{\sim}{\nu}\cdot\underset{\sim}{x}}\, \psi_\mu(\underset{\sim}{x})$. This function may be expanded in Legendre polynomials, that is,

$$D(\underset{\sim}{x}) = \sum_{L=0}^{\infty} (-i)^L (2L+1)\, D_L(x)\, P_L(\hat{\nu}\cdot\hat{x}). \tag{23}$$

Since the muons are always captured from the 1s state, the angular dependence on the right-hand side of Eq. (22) is also easily handled. Expanding the plane wave there in spherical harmonics and using Eq. (18) for the angular dependence of the Green's function, we find that

$$D_L(x) = -(\kappa^2+\nu^2)\int_0^{\infty} dx'\, x'^2\, g_L(x,x')\, j_L(\nu x')\, \psi_\mu(x'), \tag{24}$$

where j_ℓ is a spherical Bessel function of order ℓ. Assuming the muon wave function to be a constant and g_ℓ to be that for a free particle, we have $D_\ell(x) = j_\ell(\nu x)\psi_\mu(0)$, as may readily be demonstrated by carrying out the radial integral in Eq. (24). The implication of Eq. (23) for nuclear model calculations is clear. One merely replaces $j_\ell(\nu x)R_\mu(x)$ by $D_\ell(x)$. The expansion of $D(\underset{\sim}{x})$ in Eq. (23) is reminiscent of a partial wave expansion which incorporates the distortion effects of an optical potential. The important difference is that the radial functions in Eq. (23) are determined from Eq. (24) instead of solving a differential equation appropriate for the optical potential. The forms of Eqs. (22) and (24) are not changed if one introduces a local, spherically symmetric, optical potential in Eq. (17) to approximate effects of nuclear strong interactions.

4. NUMERICAL RESULTS

In this section we present numerical results for the Coulomb corrections. In order to simplify our presentation, we first isolate the various physical effects and then we consider them in combination. This requires three separate cases. First, we take the muon wave function to be a constant, and thus isolate the correction due to the distortion of the pion propagator by the nuclear Coulomb field. Second, we take the pion propagator to be that for a free particle, and thus isolate the correction due to the variation of the muon wave function over the nuclear volume. This correction is essentially an average of the Fourier transform of the pion propagator over the momentum distribution associated with the bound state muon wave function. Finally, we consider the two effects simultaneously and determine when it suffices to take the product of the results for the two corrections.

Before discussing the solution of the radial equation, we show that the distortion of the pion propagator by the static nuclear magnetic field is small in comparison with that of the nuclear Coulomb field. This assertion may be established by examining the change in the first term of Eq. (17) which results from the minimal substitution $\underset{\sim}{\nabla} \to \underset{\sim}{\nabla} - ie\underset{\sim}{A}$, where $\underset{\sim}{A}$ is the nuclear vector potential. This vector potential[17)] is approximately given by $\underset{\sim}{A}(\underset{\sim}{x}) = \underset{\sim}{\mu} \times \underset{\sim}{x}/x^3$, where $\underset{\sim}{\mu}$ is the nuclear magnetic moment and $\underset{\sim}{x}$ is measured from the nuclear center. The nuclear magnetic moment is never greater than a few nuclear magnetons, and hence the magnitude of $e\underset{\sim}{A}$ is comparable to $e^2/(2MR^2)$, where R is the nuclear radius. This number is never much greater than 0.02 MeV. For comparison, the action of the gradient operator in Eq. (17) gives rise to a term of order κ since the Green's function does not differ too much from that of a free pion (as we show below). The ratio of these two terms is thus about 2×10^{-4}, and the effect of the nuclear magnetic field is completely negligible. The magnitude of the Coulomb potential in Eq. (17) is of the order of a few MeV or a few tens of MeV.

The solution of Eq. (19) for the radial Green's function is straightforward. It may be written in terms of the solutions of the homogeneous equation,

$$\left[\frac{d^2}{dx^2} - \frac{l(l+1)}{x^2} + \left\{E - V_c(x)\right\}^2 - m_\pi^2\right] u_l(x) = 0, \tag{25}$$

as follows:

$$g_l(x,x') = \frac{u_l(x_<)\, w_l(x_>)}{x x' \left[\, u_l(x)\, w_l'(x) - u_l'(x)\, w_l(x) \,\right]}, \tag{26}$$

where $u_\ell(x)$ is the solution of Eq. (25) that is regular at the origin and w_ℓ is the solution that is bounded as $x \to \infty$. In Eq. (26) the symbol $x_<$ denotes the smaller of the two quantities x and x', and $x_>$ denotes the larger. The quantity in brackets in the denominator of Eq. (26) is the Wronskian of the two linearly independent solutions. It is independent of x.

The nucleus is taken to be a uniformly charged sphere with a radius $R = 1.2\, A^{1/3}$ fm, where A is the mass number*). Thus the Coulomb potential is given by

$$V_c(x) = -\frac{3}{2}\frac{Z\alpha}{R}\left(1 - \frac{1}{3}\frac{x^2}{R^2}\right), \qquad 0 \le x \le R;$$

$$V_c(x) = -\frac{Z\alpha}{x}, \qquad R \le x; \tag{27}$$

---

*) We choose A = 2Z if Z ≤ 25. Otherwise we use the relation between A and Z from A.E.S. Green, Nuclear physics (McGraw-Hill, Inc., New York, 1955).

where α is the fine structure constant. We solve Eq. (25) numerically using the Fox-Goodwin method[18]. For the step width and the interval for the variable x we choose h = 0.05 fm and $0 \leq x \leq 25.0$ fm, respectively.

In Fig. 2 we present results for the correction F(0) that were obtained with the potential of Eq. (27) for several values of the neutrino momentum. The muon wave function in Eq. (22) was assumed to be a constant. As one would expect, for a given neutrino momentum the size of the correction increases as Z increases. For a given value of Z, the momentum dependence of the correction may be understood directly from Eq. (17), since the importance of the term linear in the Coulomb potential decreases as the pion energy decreases. In Fig. 3 we present results for F(0) obtained by assuming the nucleus to be a point charge. The curves there all increase sharply near $Z\alpha = \frac{1}{2}$, where singular behavior is expected[19]. The curves there do not extend beyond $Z\alpha = \frac{1}{2}$ since the radial functions become ambiguous beyond this point. A comparison of Figs. 2 and 3 reveals that the differences are significant for all values of Z and are especially pronounced at large Z. For example, at ν = 20 MeV/c and Z = 20, from Fig. 2 we have F(0) = 1.13 and from Fig. 3 we have F(0) = 1.30.

At low Z we may compare the results of Fig. 3 with Baba's[13] results for the point charge. Baba did not include the term involving V_c^2 in Eq. (17). He also suggested that one could approximate the effects of finite nuclear size if one made the replacement $Z \rightarrow Z_{eff}$ [20]. If we correct Baba's results for lowest-order relativistic effects, then our numerical results for the point charge case agree with his to about four significant figures. For example, if ν = 80 MeV/c and Z_{eff} = 10.72 Baba obtains F(0) $\cong$ 1.027. Adding the lowest-order relativistic correction obtained from an analytic expression for the Green's function yields F(0) $\cong$ 1.034. Our numerical result for this value of Z_{eff} is F(0) = 1.034. This agreement furnishes an important check on our numerical work. However, <u>we do not find the use of Z_{eff} in place of Z to be an adequate approximation for considering the effects of finite nuclear size</u>. For example, in the case of 20 MeV neutrinos emitted following a muon capture by Cu (Z = 28), we have F(0) = 1.51 from the appropriate curve of Fig. 3. Using Z_{eff} = 21.16, Baba obtains F(0) $\cong$ 1.28. If we include the lowest-order relativistic correction, Baba's result is modified to F(0) $\cong$ 1.32. These numbers should be compared with F(0) = 1.18, the result for finite charge radius. Thus the use of Z_{eff} suggests a significant reduction of the correction due to finite nuclear size, but results obtained in this manner are not quantitatively reliable. This observation is not surprising since the finite size effects considered by Z_{eff} are mainly those for the muon wave function, which are not necessarily related to those for off-mass-shell pions.

Next we take the pion propagator to be that for a free particle. We calculate the muon wave function by solving numerically the Dirac equation for the 1s radial functions[21] and approximate the non-relativistic muon radial function implicit in Eq. (22) as the larger of the two relativistic radial functions. The nuclear charge distribution is assumed to have the standard functional form, namely

$$\rho(r) = \rho_0 \left[1 + e^{(r-\bar{C})/a}\right]^{-1}, \tag{28}$$

where ρ_0 is the normalization constant, a is the diffuseness, and $\bar{C}$ is the nuclear radius. For our calculation it suffices to take $a = 0.60$ fm for all nuclei and $\bar{C} = 1.2\ A^{1/3}$ fm, since we are not interested in detailed agreement of the muonic energy eigenvalues with experiment. Our results for F(0) obtained from Eq. (22) are displayed in Table 1. For comparison, results based on a point charge are also shown in Table 1. These were obtained from[13]

$$F(0) \simeq (\nu^2 + K^2)/(\nu^2 + (K + Z\alpha m_\mu)^2). \tag{29}$$

The differences are remarkably large. One may understand the origin of these differences on the basis of Fig. 4, where muonic wave functions for Z = 17 and Z = 50 are depicted. The large differences of Table 1 are a consequence of the large differences of the slopes dashed and full curves near the origin.n. Reliable results for intermediate values of Z and ν may be obtained from those of Table 1 by interpolation.

Now we study simultaneously the two effects discussed above. In Table 2 we present results for F(0) obtained with the distorted pion propagator and muon wave functions based on the charge distribution of Eq. (28). Considerable cancellation between the two effects is evident, as noted by Baba[13]. One may obtain a reliable results for both effects simply by multiplying the appropriate result of Fig. 2 with that of Table 1, provided that neither correction is very large. For instance, if we do this for Z = 30 and ν = 60 MeV/c, we find F(0) $\cong$ 0.99, which is very close to the corresponding result in Table 2. If we do this for Z = 80 and ν = 20 MeV/c, we find F(0) $\cong$ 1.23, a number about 10% larger than the corresponding entry in Table 2. Thus some interference between the two effects is apparent here.

Unfortunately, the numbers presented in Table 2 are not sufficient for a quantitatively accurate calculation of the importance of the Coulomb correction, since this correction varies somewhat over the nuclear volume. To emphasize this point, we present, in Figs. 5 and 6, results for $\sqrt{4\pi}\, D_0(r)$ and $\sqrt{4\pi}\, D_1(r)$, which were calculated using Eq. (24). These are compared with $\sqrt{4\pi}\, \psi_\mu(0) j_0(\nu r)$ and $\sqrt{4\pi}\, \psi_\mu(0) j_1(\nu r)$. From these figures it is apparent that the functions D_ℓ are distorted relative to the spherical Bessel functions. This distortion seems to vary in a rather complicated way as the neutrino energy varies. The amount of distortion also depends upon the angular momentum, as reflected in a comparison of Figs. 5b and 6. Thus the numbers presented in Table 2 must be thought of as only a rough estimate of the correction. In order to treat the Coulomb corrections reliably, one must use the functions $D_\ell(x)$ in a nuclear model calculation. Fortunately, the correction may be small enough to be ignored in most cases. It would seem to be premature to do a model-dependent calculation until the effects of nuclear strong interactions can be included in D_ℓ.

5. APPROXIMATE METHODS

In this section we develop two approximate methods for obtaining the results of Section 4. We pay particular attention to the ranges of validity of these techniques. The purpose of this endeavor is threefold. First, we wish to present analytic expressions for the corrections from which rapid calculations of the corrections can be made. Second, we want to have a further means for checking the numerical work, and finally, certain features of the results will be transparent when viewed in the context of these methods. Furthermore, it may be possible to extend these methods so that they are useful when the effects of nuclear strong interactions on the pion are included.

We first consider the correction due to the variation of the muon wave function over the nuclear volume. We calculate F(0) in order to make a comparison with the numerical results of Table 1. Setting $\underset{\sim}{x} = 0$ in Eq. (22), using the expression

$$G^F_{E_\pi}(0, \underset{\sim}{x}') = -e^{-\kappa x'}/4\pi x' \tag{30}$$

for the free pion propagator there and doing the angular integration there, we find that

$$F(0) = [\nu\,\psi_\mu(0)]^{-1} \times (\kappa^2+\nu^2)\int_0^\infty dx'\, e^{-\kappa x'} \sin\nu x'\, \psi_\mu(x'). \tag{31}$$

In order to obtain F(0) from this expression it is not necessary to know the value of the muon wave function at the origin; it is only necessary to know the variation of the muon wave function over the nuclear volume relative to its value at the origin. This may be obtained from a power series solution of the Schrödinger equation valid near the origin and the experimental values of the muonic 1s energy eigenvalue without solving the eigenvalue problem. The power series solution takes the form

$$\psi_\mu(x') = \psi_\mu(0) \sum_{n=0}^\infty B_n x'^n, \tag{32}$$

where $B_0 = 1.0$ and the remaining B_n depend upon the functional form of the nuclear charge distribution. If the nucleus is approximated as a uniformly-charged sphere, then $B_1 = B_3 = 0$, and

$$B_2 = -\frac{1}{3} m_\mu \left(E_\mu + \frac{3}{2}\frac{Z\alpha}{R} \right),$$

$$B_4 = \frac{Z\alpha m_\mu}{20 R^3} + \frac{1}{30} m_\mu^2 \left(E_\mu + \frac{3}{2}\frac{Z\alpha}{R} \right)^2, \tag{33}$$

where E_μ is the binding energy of the muon. Substituting Eq. (32) into Eq. (31), and using the identity

$$x'^n e^{-Kx'} = (-)^n \left(\frac{\partial}{\partial K}\right)^n e^{-Kx'}, \tag{34}$$

yields the expression

$$F(0) = \frac{K^2+\nu^2}{\nu^2} \sum_{n=0}^{\infty} (-)^n B_n \left(\frac{\partial}{\partial K}\right)^n \int_0^\infty dx' e^{-Kx'} \sin \nu x'. \tag{35}$$

Carrying out the x' integration in Eq. (35), we have

$$F(0) = (K^2+\nu^2) \sum_{n=0}^{\infty} (-)^n B_n \left(\frac{\partial}{\partial K}\right)^n \frac{1}{(K^2+\nu^2)}. \tag{36}$$

This equation is a useful result provided that the sum in Eq. (36) converges rapidly.

Results based on the first five terms (two of which are zero) of Eq. (36) with the coefficients B_i given by Eqs. (33) are displayed in Table 3. These numbers never differ from their counterparts in Table 1 by more than 2%. These differences arise mainly from the use of different nuclear charge distributions, and the first five terms of Eq. (36) represent an entirely adequate approximation. It is instructive to compare this with the point charge case, where $\psi(x') = \psi(0)\ e^{-Z\alpha m_\mu x'}$. Then the coefficients $B_n = (Z\alpha m_\mu)^n/n!$ and one can readily see that Eq. (36) is the power series expansion of the result of Eq. (29). However, many more than six terms are required in order to obtain reliable results for large Z. Thus the more rapid variation of the muonic wave function in the point charge case not only leads to a gross overestimate of the magnitude of the effect of averaging over the muon momenta, but also leads to a breakdown of approximations that suffice for the finite charge radius case. On the basis of Eqs. (33) and (36), it is also easy to understand the slow variation of the correction with Z (for the case of finite charge radius). The largest part of the correction comes from the term involving B_2. As the first of Eqs. (33) shows, the Z dependence of B_2 results from a sum involving the binding energy and $3Z\alpha/2R$. The Z dependence of these two terms tends to cancel for intermediate and large values of Z, and hence B_2 varies more slowly than one might expect.

The remainder of our study of approximation methods will be based on a differential equation for the function $F(\underset{\sim}{x})$. The motivation for this approach is a desire to circumvent the construction of the Green's function for the nuclear Coulomb field. It will turn out that the exact solution of the differential equation is probably a more formidable task than the exact calculation of $F(\underset{\sim}{x})$ from Eq. (22), but the differential equation is a more convenient starting point for approximate treatments. For obtaining the differential equation, we begin by rewriting Eq. (22) in the form,

$$F(\underset{\sim}{x}) = T(\underset{\sim}{x}) \int d^3x' \, G_{E_\pi}(\underset{\sim}{x}, \underset{\sim}{x}') \, e^{-i \underset{\sim}{\nu} \cdot \underset{\sim}{x}'} \psi_\mu(\underset{\sim}{x}'), \tag{37}$$

where $T(\underset{\sim}{x}) = -(\kappa^2 + \nu^2) \, e^{i\underset{\sim}{\nu}\cdot\underset{\sim}{x}}/\psi_\mu(\underset{\sim}{x})$. Taking two derivatives of Eq. (37), we have

$$\begin{aligned} \nabla^2 F(\underset{\sim}{x}) = {} & [\nabla^2 T(\underset{\sim}{x})] \int d^3x' \, G_{E_\pi}(\underset{\sim}{x}, \underset{\sim}{x}') \, e^{-i \underset{\sim}{\nu} \cdot \underset{\sim}{x}'} \psi_\mu(\underset{\sim}{x}') \\ & + 2 \underset{\sim}{\nabla} T(\underset{\sim}{x}) \cdot \int d^3x' \, \underset{\sim}{\nabla} G_{E_\pi}(\underset{\sim}{x}, \underset{\sim}{x}') \, e^{-i \underset{\sim}{\nu} \cdot \underset{\sim}{x}'} \psi_\mu(\underset{\sim}{x}') \\ & + T(\underset{\sim}{x}) \int d^3x' \, \nabla^2 G_{E_\pi}(\underset{\sim}{x}, \underset{\sim}{x}') \, e^{-i \underset{\sim}{\nu} \cdot \underset{\sim}{x}'} \psi_\mu(\underset{\sim}{x}'). \end{aligned} \tag{38}$$

We indicate briefly how one handles each of the three terms on the right-hand side of Eq. (38). In the first term one uses the definition of $T(\underset{\sim}{x})$ in order to write $\nabla^2 T(\underset{\sim}{x})$ as a product of $T(\underset{\sim}{x})$ and a factor containing derivatives of neutrino and muon wave functions. Then using Eq. (37) one may write the first term as a product of this factor and $F(\underset{\sim}{x})$. One handles the $\underset{\sim}{\nabla} T(\underset{\sim}{x})$ in the second term in a manner similar to that for handling $\nabla^2 T(\underset{\sim}{x})$ in the first term. To evaluate the second factor in the second term one divides Eq. (37) by $T(\underset{\sim}{x})$ and takes the gradient of both sides. Thus from the second term in Eq. (38), terms involving both $\underset{\sim}{\nabla} F$ and F emerge. To evaluate the third term one must use Eq. (17) for the pion Green's function. The differential equation thus derived is

$$\begin{aligned} \nabla^2 F(\underset{\sim}{x}) = {} & \left[\nu^2 + m_\pi^2 - (E_\pi - V_c)^2 + \frac{2i\underset{\sim}{\nu} \cdot \underset{\sim}{\nabla} \psi_\mu(x)}{\psi_\mu(x)} - \frac{\nabla^2 \psi_\mu(\underset{\sim}{x})}{\psi_\mu(\underset{\sim}{x})} \right] F(\underset{\sim}{x}) \\ & + 2 \left[i\underset{\sim}{\nu} - \frac{\underset{\sim}{\nabla} \psi_\mu(x)}{\psi_\mu(x)} \right] \cdot \underset{\sim}{\nabla} F(\underset{\sim}{x}) \\ & - \kappa^2 - \nu^2. \end{aligned} \tag{39}$$

The source term in Eq. (39) arises from the third term of Eq. (38) when one replaces the factor $\nabla^2 G_{E_\pi}$ by that part of Eq. (17) involving the delta function.

Under the assumption that the muon wave function is a constant, Eq. (39) reduces to

$$\nabla^2 F(\underset{\sim}{x}) = [\nu^2 + m_\pi^2 - (E_\pi - V_c)^2]\, F(\underset{\sim}{x}) + 2i\, \underset{\sim}{\nu}\cdot\underset{\sim}{\nabla} F(\underset{\sim}{x}) - K^2 - \nu^2. \tag{40}$$

We note that if $V_c = 0$, then $F(\underset{\sim}{x}) = 1$ is a particular solution of Eq. (40). This fact suggests an approximate method of solving Eq. (40). It is based on the assumption that $F(\underset{\sim}{x})$ is slowly varying, so that the derivatives of F in Eq. (40) make small contributions in comparison with F. We further assume the second derivative term to be small in comparison with the first derivative term. We write $F(\underset{\sim}{x}) = F^{(0)}(\underset{\sim}{x}) + F^{(1)}(\underset{\sim}{x}) + F^{(2)}(\underset{\sim}{x}) + \ldots$, where the superscripts refer to the order of smallness. Substituting this expression into Eq. (40) and equating terms of the same order of smallness, we find that

$$F^{(0)}(\underset{\sim}{x}) = \frac{K^2+\nu^2}{\nu^2 + m_\pi^2 - (E_\pi - V_c(x))^2},$$

$$F^{(1)}(\underset{\sim}{x}) = \frac{-2i\,\underset{\sim}{\nu}\cdot\underset{\sim}{\nabla} F^{(0)}(\underset{\sim}{x})}{\nu^2 + m_\pi^2 - (E_\pi - V_c(x))^2},$$

$$F^{(2)}(\underset{\sim}{x}) = \frac{\nabla^2 F^{(0)}(x) - 2i\,\underset{\sim}{\nu}\cdot\underset{\sim}{\nabla} F^{(1)}(\underset{\sim}{x})}{\nu^2 + m_\pi^2 - (E_\pi - V_c(x))^2}. \tag{41}$$

From these equations it is easy to see how the angular momentum dependence and the variation of the correction over the nuclear volume arise. The fact that we found the angular momentum dependence to be slight in Section 4 can be viewed as evidence in favor of this approximate method of solving Eq. (40). In order to ascertain the domain of validity of Eqs. (41), we choose the Coulomb potential of Eq. (27) and evaluate the derivatives in Eqs. (41). Setting $\underset{\sim}{x} = 0$ we find

$$F^{(0)}(0) = \frac{K^2+\nu^2}{\nu^2 + m_\pi^2 - (E_\pi + 3Z\alpha/2R)^2},$$

$$F^{(1)}(0) = 0,$$

$$F^{(2)}(0) = \frac{(K^2+\nu^2)(E_\pi + 3Z\alpha/2R)\, Z\alpha}{R^3[\nu^2 + m_\pi^2 - (E_\pi + 3Z\alpha/2R)^2]^3} \times \left[-6 + \frac{8\nu^2}{\nu^2 + m_\pi^2 - (E_\pi + 3Z\alpha/2R)^2}\right]. \tag{42}$$

Acknowledgements

This work was started when both authors were at the University of Maryland, and the numerical computations reported in this work were funded by the University of Maryland Computer Center. We are thankful to Professor M.K. Banerjee for originally emphasizing the importance of the nuclear finite size effects and for many stimulating discussions in the early stage of the work. We also are grateful to Professors J.M. Eisenberg, M. Ericson, T.E.O. Ericson, W.M. MacDonald, M.H. Macfarlane, A. Sirlin, and to Dr. F. Cannata for important discussions. We thank Dr. K. Baba, for a valuable correspondence regarding his work, Professor J. Deutsch and Dr. L. Palffy, for communicating their results prior to publication. One of us (N.C.M.) gratefully acknowledges the CERN hospitality.

REFERENCES

1) J.D. Walecka *in* Muon physics, eds. V.W. Hughes and C.S. Wu, to be published.
N.C. Mukhopadhyay, Selected aspects of nuclear muon capture, to be published in Physics Reports.

2) J.M. Eisenberg and W. Greiner, Excitation mechanisms of the nucleus (North-Holland Publ. Co., Amsterdam, 1970), Vol. II, p. 313.

3) M. Gell-Mann and M. Lévy, Nuovo Cimento 16 (1960) 705.
V. de Alfaro, S. Fubini, G. Furlan and C. Rosetti, Currents in hadron physics (North-Holland Publ. Co., Amsterdam, 1973), pp. 173 ff.

4) A. Alberigi Quaranta, A. Bertin, G. Matone, F. Palmonari, G. Torelli, P. Dalpiaz, A. Placci and E. Zavattini, Phys. Rev. 177 (1969) 2118.

5) E. Peterson, Phys. Rev. 167 (1968) 971.
N.C. Mukhopadhyay and M.H. Macfarlane, Phys. Rev. Letters 27 (1971) 1823.
J. Bernabeu, Nuovo Cimento 4 A (1971) 715.
N.C. Mukhopadhyay, Phys. Letters 40 B (1972) 157; ibid. 44 B (1973) 33.
J. Vergados, Nuclear Phys. A220 (1974) 259.

6) L. Palffy, Thèse, IPC-N-7404, Université Catholique de Louvain (unpublished), 1974; and to be published.

7) J.P. Deutsch, L. Grenacs, J. Lehmann, P. Lipnik and P.C. Macq, Phys. Letters 29 B (1969) 66.

8) F.R. Kane, M. Eckhause, G.H. Miller, B.L. Roberts, M.E. Vislay and R.E. Welsh, Phys. Letters 45 B (1973) 292.

9) L.M. Rosenstein and I.S. Hammerman, Phys. Rev. C8 (1973) 603.

10) H. Ohtsubo, Phys. Letters 22 (1966) 480.
J. Delorme and M. Rho, Phys. Letters 34 B (1971) 238.
M. Ericson, A. Figureau and C. Thévenet, Phys. Letters 45 B (1973) 19.
N.C. Mukhopadhyay and L.D. Miller, Phys. Letters 47 B (1973) 415.
D.H. Wilkinson, Phys. Letters 48 B (1974) 169.
M. Rho, Stony Brook preprint, May 1974.

11) L.P. Fulcher and N.C. Mukhopadhyay, Bull. Amer. Phys. Soc. 18 (1973) 676; ibid. 19 (1974) 577; Phys. Letters 47 B (1973) 115.

12) A.M. Green and M. Rho, Nuclear Phys. A130 (1969) 112.
J.B. Cammarata and M.K. Banerjee, Phys. Rev. Letters 31 (1973) 610.
J. Delorme, M. Ericson and G. Fäldt, to be published.
F. Cannata and N.C. Mukhopadhyay, to be published.

13) K. Baba, Progr. Theor. Phys. 43 (1970) 390.

14) L.D. Blokhintsev and E.I. Dolinsky, Nuclear Phys. 34 (1962) 498.

15) J.M. Eisenberg and W. Greiner, Microscopic theory of the nucleus (North-Holland Publ. Co., Amsterdam, 1972), Vol. III, p. 110.

16) D. Tadić, Nuclear Phys. 26 (1961) 338.

17) J.D. Jackson, Classical electrodynamics (John Wiley & Sons, Inc., New York, 1962) p. 79 and p. 146.

18) L. Fox and E.T. Goodwin, Proc. Cambridge Phil. Soc. 45 (1949) 373.

19) K.M. Case, Phys. Rev. 80 (1950) 797.

20) J.C. Sens, Phys. Rev. 113 (1959) 679.

21) M.E. Rose, Relativistic electron theory (John Wiley & Sons, Inc., New York, 1961) p. 160.

Table 1

Corrections due to the momentum distribution of the muon. F_p is the point charge result and F_e is based on a Fermi charge distribution.

Z	ν = 100 MeV/c		ν = 60 MeV/c		ν = 20 MeV/c	
	F_p	F_e	F_p	F_e	F_p	F_e
10	0.93	0.98	0.91	0.97	0.88	0.94
20	0.87	0.97	0.83	0.94	0.78	0.91
30	0.81	0.96	0.76	0.93	0.69	0.88
40	0.76	0.95	0.70	0.92	0.62	0.87
50	0.71	0.95	0.65	0.91	0.57	0.86
60	0.66	0.95	0.60	0.91	0.52	0.85
70	0.62	0.95	0.56	0.91	0.48	0.85
80	0.58	0.95	0.52	0.91	0.45	0.85
90	0.55	0.94	0.49	0.90	0.42	0.84
100	0.52	0.94	0.46	0.90	0.39	0.84

Table 2

Corrections due to both the momentum distribution of the muon and the distortion of the pion propagator

Z	F(0)		
	ν = 100 MeV/c	ν = 60 MeV/c	ν = 20 MeV/c
10	0.98	0.99	1.00
20	0.97	0.98	1.01
30	0.97	0.98	1.02
40	0.96	0.98	1.04
50	0.96	0.99	1.06
60	0.96	0.99	1.07
70	0.96	0.99	1.09
80	0.96	0.99	1.11

Table 3

Approximate values for the correction due to muon momentum distribution

Z	F(0)		
	ν = 100 MeV/c	ν = 60 MeV/c	ν = 20 MeV/c
20	0.96	0.94	0.93
40	0.95	0.92	0.89
60	0.95	0.91	0.87
80	0.94	0.90	0.87

Table 4

Approximate values for the correction due to the distortion of the pion propagator for Z = 20

ν (MeV/c)	$F^{(0)}(0)$	$F^{(0)}(0) + F^{(2)}(0)$	F(0)
100	1.008	1.007	1.007
80	1.026	1.023	1.023
60	1.054	1.043	1.044
40	1.098	1.068	1.076
20	1.180	1.087	1.126
10	1.256	1.071	1.166

Table 5

Approximate values for the correction due to the distortion of the pion propagator for Z = 80

ν (MeV/c)	$F^{(0)}(0)$	$F^{(0)}(0) + F^{(2)}(0)$	F(0)
100	1.031	1.029	1.029
80	1.080	1.075	1.075
60	1.157	1.143	1.144
40	1.297	1.251	1.258
20	1.625	1.407	1.483
10	2.041	1.328	1.703

Table captions

Table 1 : Corrections due to the momentum distribution of the muon. F_p is the point charge result and F_e is based on a Fermi charge distribution.

Table 2 : Corrections due to both the momentum distribution of the muon and the distortion of the pion propagator.

Table 3 : Approximate values for the correction due to muon momentum distribution.

Table 4 : Approximate values for the correction due to the distortion of the pion propagator for Z = 20.

Table 5 : Approximate values for the correction due to the distortion of the pion propagator for Z = 80.

Figure captions

Fig. 1 : Graphs for the Coulomb corrections.

Fig. 2 : Coulomb corrections to the induced pseudoscalar term for a finite charge radius.

Fig. 3 : Coulomb corrections to the induced pseudoscalar term for a point charge.

Fig. 4 : 1s radial functions for muonic atoms.

Fig. 5 : The functions $\sqrt{4\pi}\, D_0(x)$ (full curves) and $\sqrt{4\pi}\, \psi_\mu(0) j_0(\nu x)$ (dashed curves) for ν = 20 MeV/c, 60 MeV/c, and 100 MeV/c.

Fig. 6 : The functions $\sqrt{4\pi}\, D_1(x)$ (full curves) and $\sqrt{4\pi}\, \psi_\mu(0) j_1(\nu x)$ (dashed curves) for ν = 60 MeV/c.

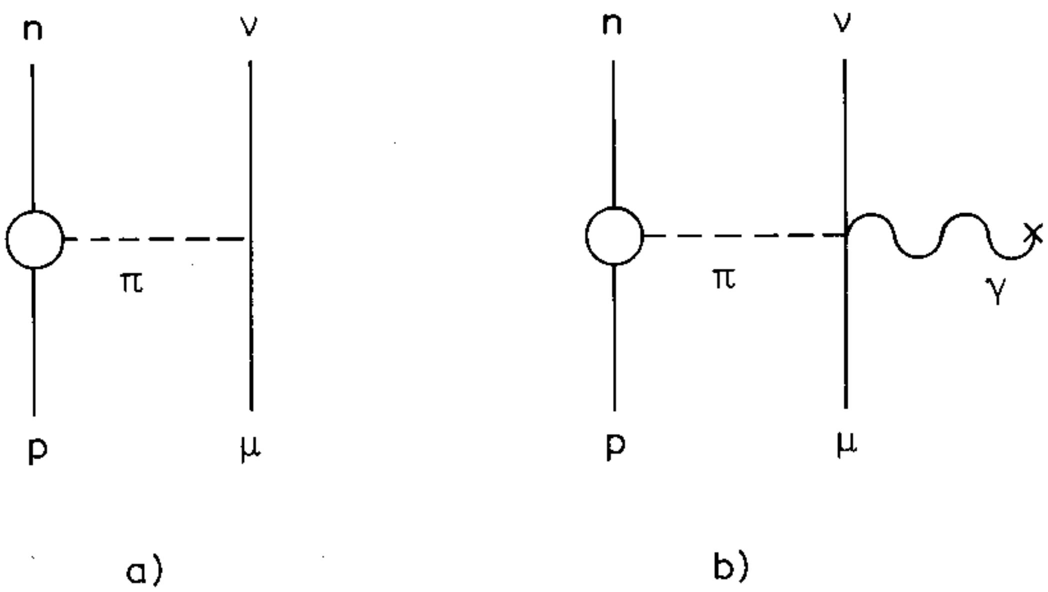

Fig. 1

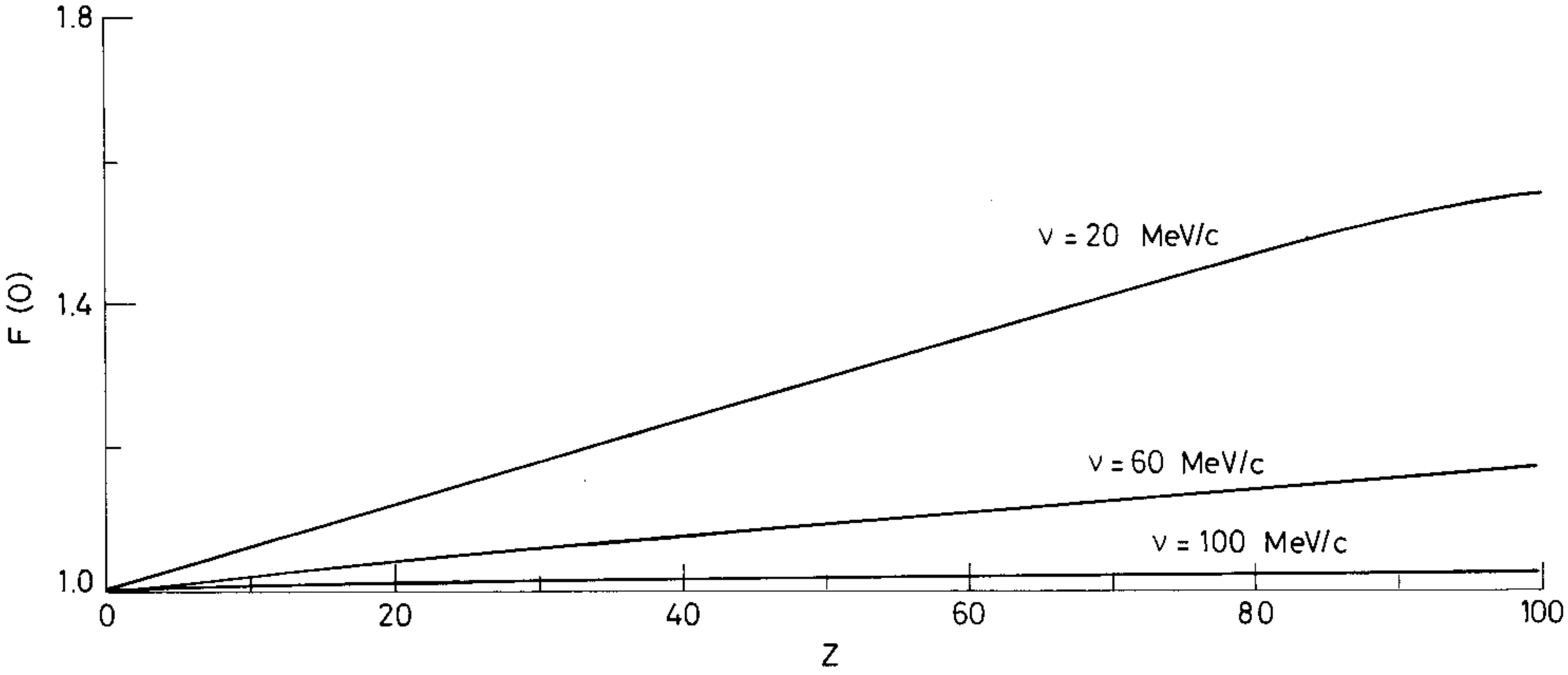

Fig. 2

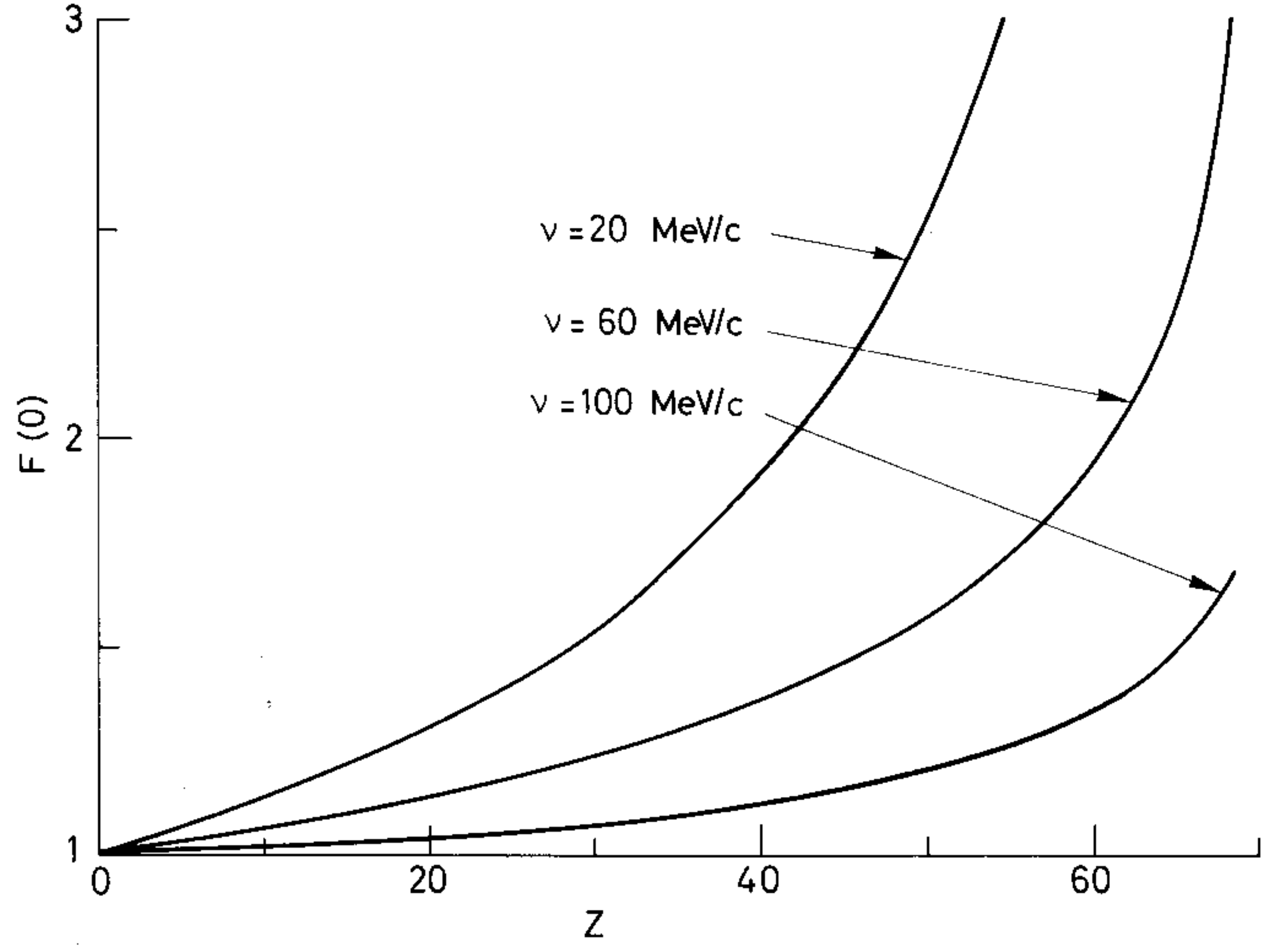

Fig. 3

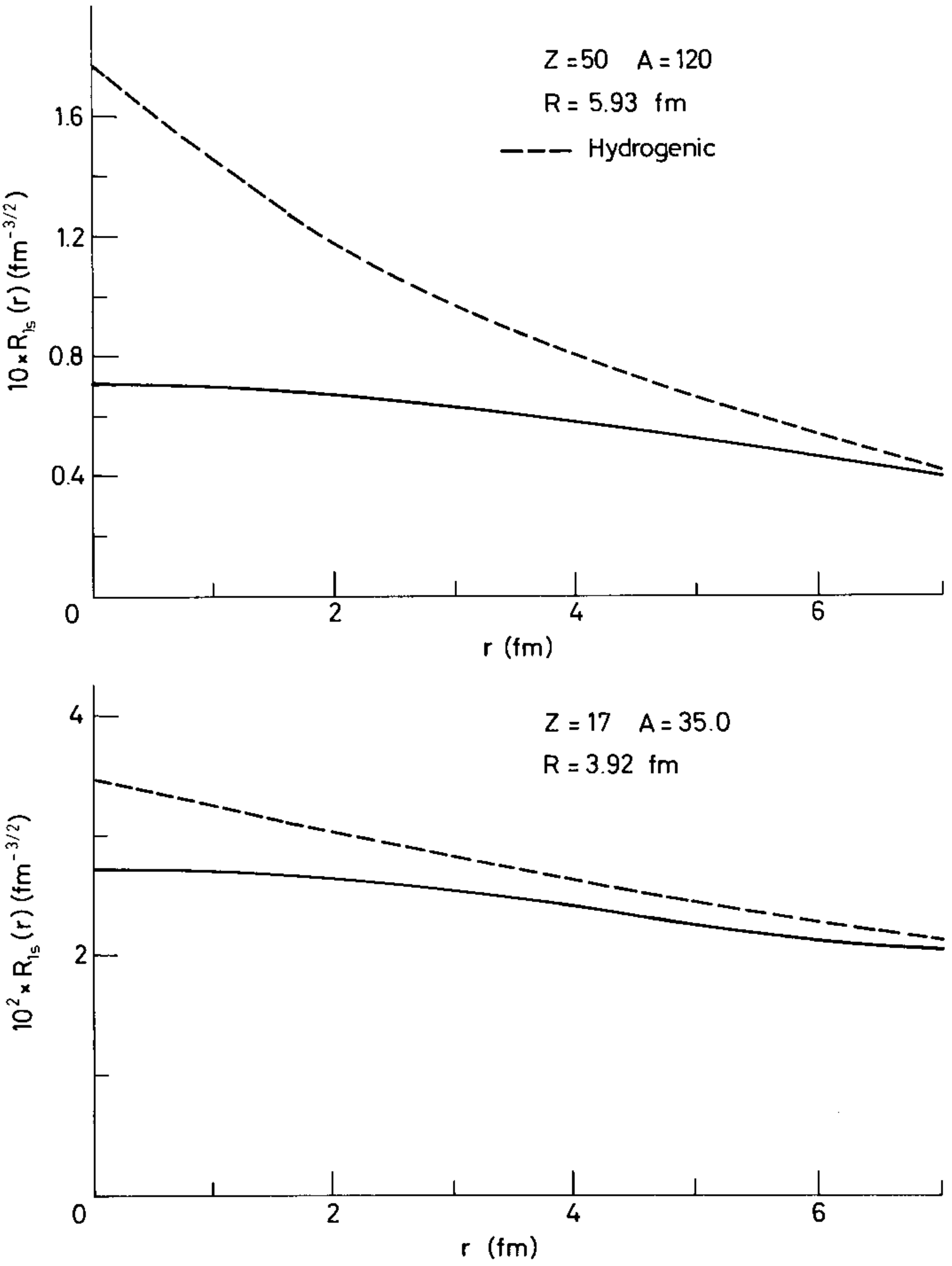
Z = 50 A = 120
R = 5.93 fm
Hydrogenic
1.6
1.2
0.8
0.4
10 × R1s (r) (fm^-3/2)
0
2
4
6
r (fm)
Z = 17 A = 35.0
R = 3.92 fm
4
2
10^2 × R1s (r) (fm^-3/2)
0
2
4
6
r (fm)

Fig. 4

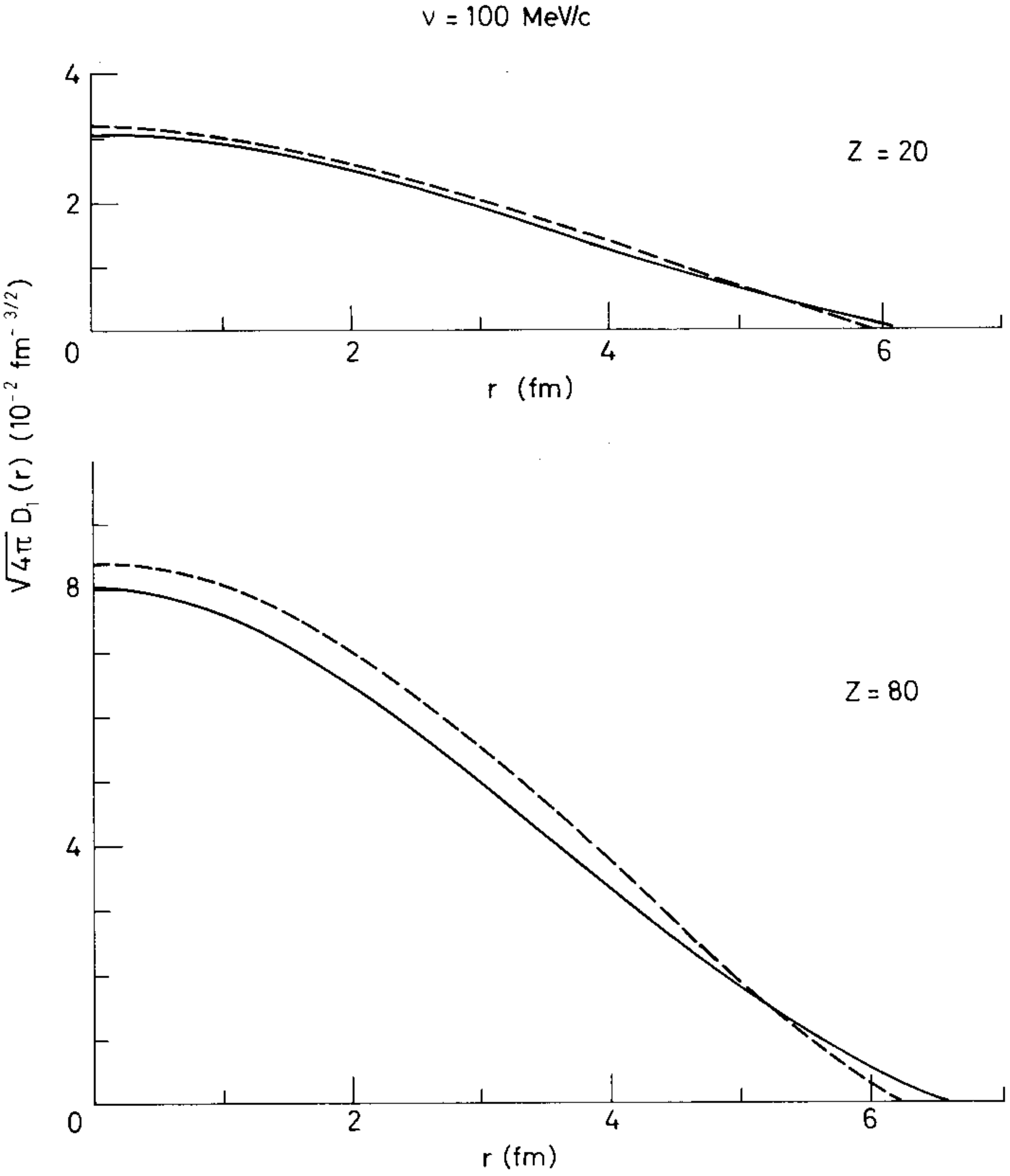

Fig. 5a

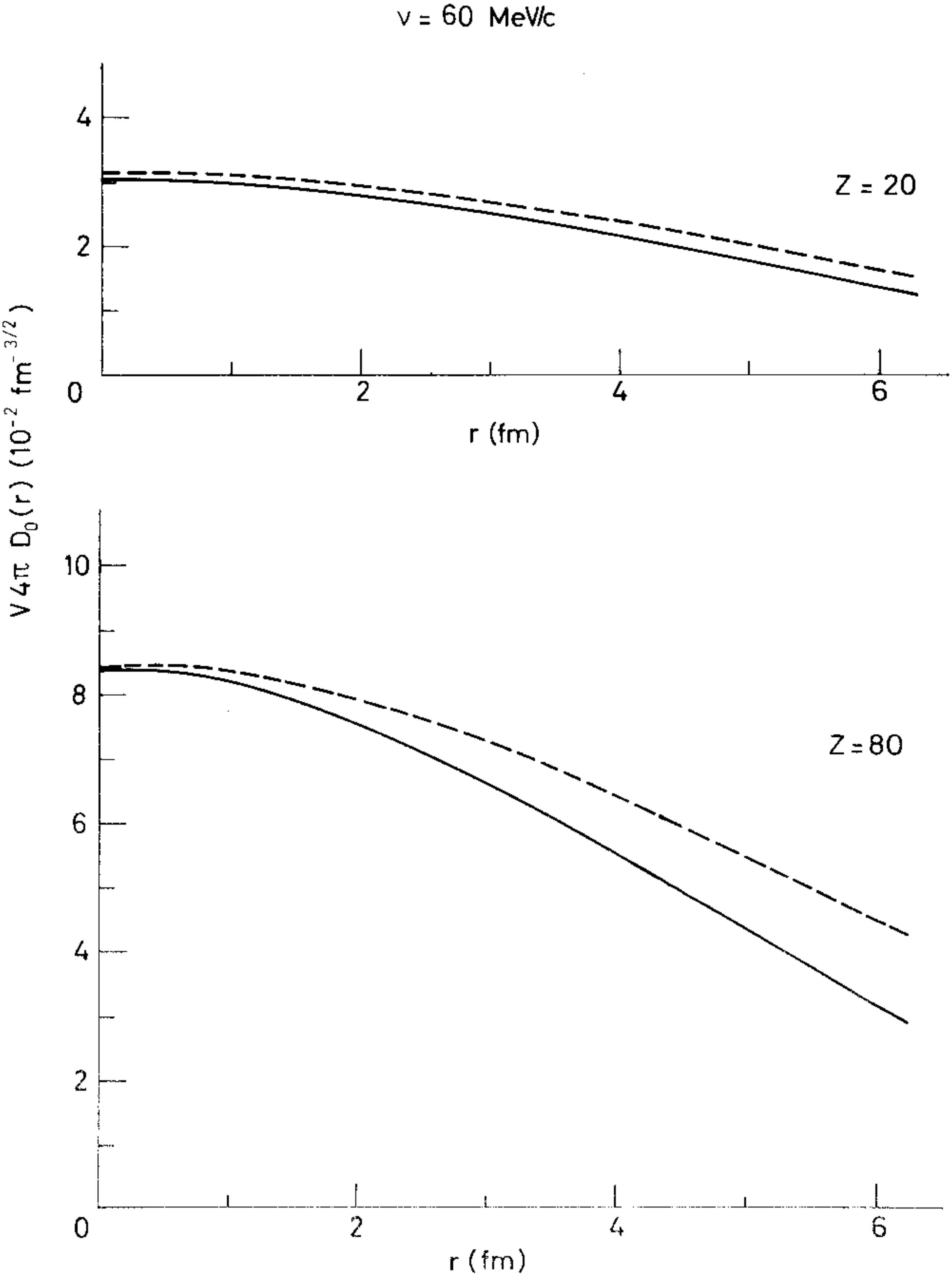
ν = 60 MeV/c
$\sqrt{4\pi}\ D_0(r)\ (10^{-2}\ fm^{-3/2})$
Z = 20
0
2
4
2
4
6
r (fm)
Z = 80
10
8
6
4
2
0
2
4
6
r (fm)

Fig. 5b

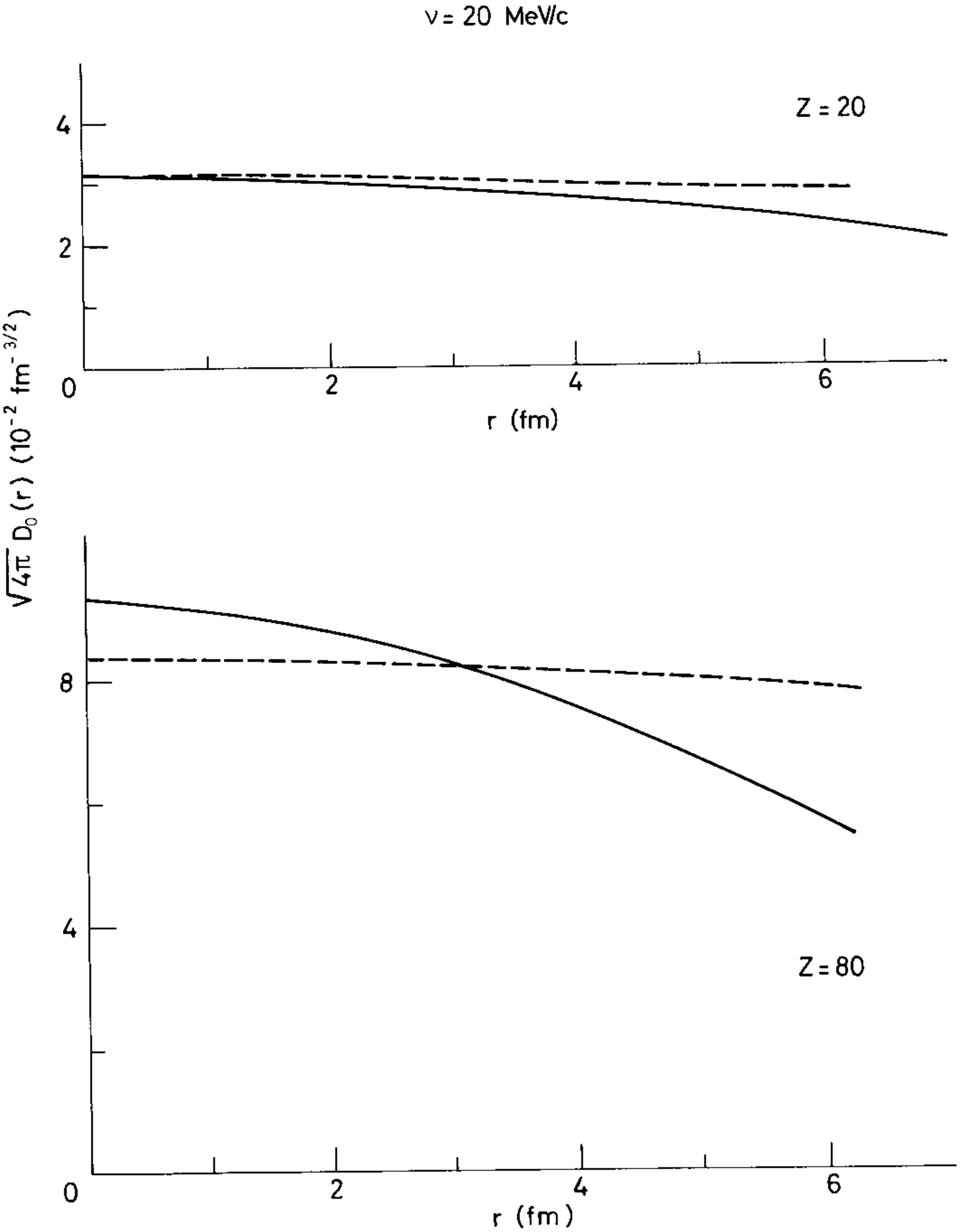

Fig. 5c

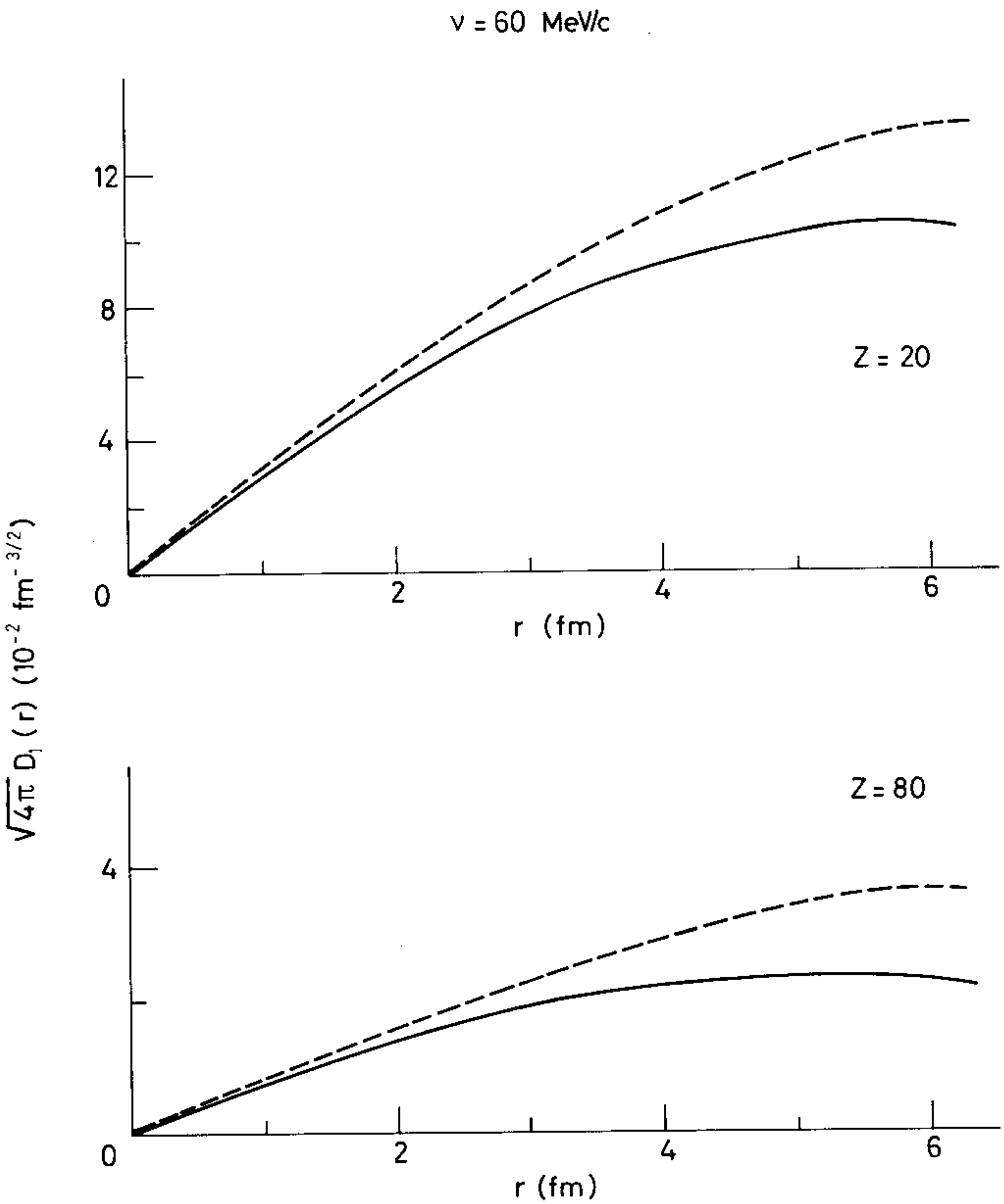

Fig. 6